DOI: 10.1002/ejic.201000007

Successive Ligand and Metal Oxidation: Redox Reactions Involving Binuclear Cu^{I} Complexes of Chelating Guanidine Ligands

Dimitri Emeljanenko,[a] Anastasia Peters,[a] Norbert Wagner,[a] Johannes Beck,[b] Elisabeth Kaifer,[a] and Hans-Jörg Himmel*[a]

Keywords: Binuclear complex / Oxidation / Copper / Guanidine / Semiconductors / Redox chemistry

New binuclear complexes of three-coordinate Cu^{I} have been synthesized with the ligand 1,2,4,5-tetrakis(tetramethylguanidino)benzene (ttmgb). Subsequent oxidation of the ligand unit was achieved by reaction with Br_2 or I_2. Reaction with Br_2 leads to oxidation of both the ligand and the copper ions and formation of a bicationic dinuclear Cu^{II} complex. On the other hand, oxidation with I_2 leads only to oxidation of the ligand during the first step. A metastable coordination polymer of ladder-type structure results, in which the coordination number of the Cu^{I} ions increases to four. Electrical measurements show that this polymer is semiconductive with a band gap of around 1 eV. The electronic structure of the polymer was further studied by X-ray photoelectron spectroscopy (XPS), Raman and Vis/NIR spectroscopy. It decomposes (with oxidation of the copper ions) in an exothermal reaction at temperatures around 230 °C. Oxidation of the copper ions and decomposition of the polymer can also be achieved by reaction of the polymer with phenanthroline.

Introduction

Coordination polymers are an exciting class of compounds, especially due to the number of different potential applications,[1–4] and, for example, conductive or semiconductive, photo- and electroluminescent, nonlinear optical, liquid crystalline, magnetic (especially those with spin-crossover behaviour) and catalytically active materials have been fabricated. Cu^{I} ions have been incorporated into a number of coordination polymers. Complexes of CuI in particular are known to form coordination polymers with a variety of different structural types that feature, for example, rhombic $[Cu_2I_2]$ or cubanelike $[Cu_4I_4]$ units.[5]

We recently developed guanidino-functionalized aromatic compounds (GFAs) as a new family of strong electron-donor compounds and complex ligands for incorporation into coordination polymers. Two representatives of this family are 1,2,4,5-tetrakis(tetramethylguanidino)benzene (ttmgb, see Scheme 1)[6] and 1,4,5,8-tetrakis(tetramethylguanidino)naphthalene (ttmgn).[7] Oxidation with I_2 gives the two salts $[ttmgb](I_3)_2$ (**1**) and $[ttmgn](I_3)_2$, the structures of which were recently reported by us.[6,7] Both GFAs have already been used to synthesize binuclear complexes of various metals, including Cu^{II}[8] and Co^{II}.[7] Herein we now report on binuclear Cu^{I} complexes of ttmgb and their oxidation reactions. Chelating guanidine ligands were already intensively studied in the past.[9,10] Harmjanz, Henkel et al. showed that 1,3-bis(tetramethylguanidino)propane can be used as a bidentate ligand in a number of complexes including Cu^{I} and Cu^{II}.[11] In addition, Tamm et al. reported on the synthesis and reactivity of some Cu^{I} complexes that feature bisguanidine ligands.[12] Reactions of some of these complexes with O_2 were analyzed, and the complexes were successfully applied as catalysts for the polymerization of styrene. Another example is the tripodal, superbasic and sterically encumbered tris(tetramethylguanidino)tren (TMG3tren) ligand, which coordinates Cu^{I} ions. A 1:1 Cu/O_2 complex featuring end-on-coordinated O_2 can be realized with this system, and this superoxo complex was shown to exhibit a rich chemistry.[13,14] In all these examples mononuclear guanidine complexes were formed.

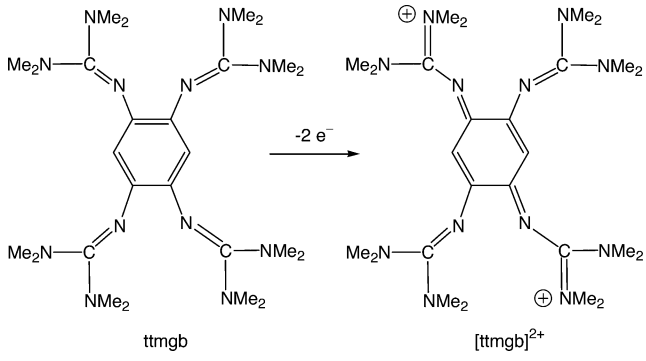

Scheme 1. Lewis formulae for the neutral and oxidized ttmgb ligand.

[a] Anorganisch-Chemisches Institut, Ruprecht-Karls-Universität Heidelberg,
Im Neuenheimer Feld 270, 69120 Heidelberg, Germany
Fax: +49-6221-545707
E-mail: hans-jorg.himmel@aci.uni-heidelberg.de
[b] Institut für Anorganische Chemie, Universität Bonn,
Gerhard-Domagk-Str. 1, 53121 Bonn, Germany
Supporting information for this article is available on the WWW under http://dx.doi.org/10.1002/ejic.201000007.

Results and Discussion

We started our work with the synthesis of the two binuclear complexes, $[(CuBr)_2(ttmgb)]$, (**2**) and $[(CuI)_2(ttmgb)]$ (**3**), by reaction of ttmgb with CuBr and CuI, respectively, in CH_3CN at 70 °C. Both compounds can be crystallized from the reaction mixture after addition of Et_2O. The molecular structures as derived from a single-crystal XRD analysis for both complexes are visualized in Figures 1 and 2 (see Tables S1 and S2 in the Supporting Information for selected structural parameters). The C–C bond lengths within the central C_6 ring in **2** and **3** vary only slightly (within the range 139.0–140.4 pm for **2** and 138.9–141.7 pm for **3**), thus showing that the aromatic system remains intact. The Cu^I ions in both complexes are tricoordinated, and the N–Cu–N bite angles are 82.89(12)° for **2** and 83.45(8)° for **3**. Interestingly, the N1–Cu–Br and N4–Cu–Br angles in **2** are, at 146.81(9) and 130.10(9)°, respectively, significantly different. With lengths of 199.2(3) and 205.9(3) pm, the two bonds established between each of the Cu ions and the imino N atoms of the ttmgb ligand in **2** also differ slightly in length in the solid state. For comparison, Herres-Pawlis et al. reported values of 202.94(14)/204.63(3) pm for the Cu–N bond lengths in the Cu^I complex of N1,N2-bis(1,3-dimethylimidazolidin-2-yliden)ethane-1,2-diamine.[15] Tamm et al. reported Cu–N bond lengths of 205.8(1)/200.2(1) pm in CuCl complexes of substituted 1,2-bis(imidazolin-2-imino)ethane.[12] At 85.22(5)°, the N–Cu–N bite angle in complex **4** is close to that in **2** or **3**. In the complex $[Cu^I(btmgp)]$ [btmgp = 1,3-bis(tetramethylguanidino)propane], Cu–N distances and N–Cu–N angles of 201.0(5)/200.2(5) and 103.3(2)° were found.[11] In solution, the dynamic behaviour of the guanidino groups[16] is responsible for the observation of only one signal for the protons of the 16 methyl groups (at δ = 2.82 for **2** and 2.92 ppm for **3**) and also only one signal for the two ring protons (at δ = 5.43 for **2** and 5.59 ppm for **3**) in the ^1H NMR spectra.

Subsequently, we reacted complex **3** with I_2. Reaction in CH_3CN at room temperature proceeded to give a new product **4** $\{[(CuI)_2(ttmgb)](I_3)_2\}_n$, see Equation (1), which crystallized from the reaction mixture after partial solvent removal. The analysis and single-crystal XRD measurements

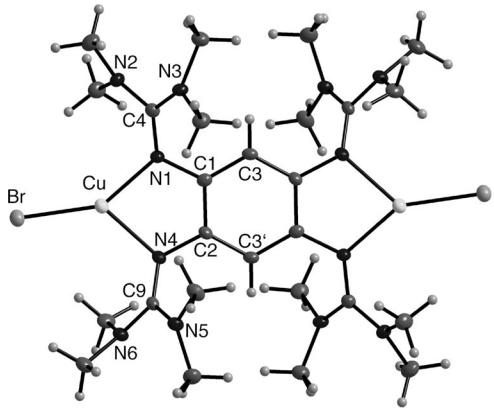

Figure 1. Molecular structure of **2**. Thermal ellipsoids are drawn at the 50% probability level.

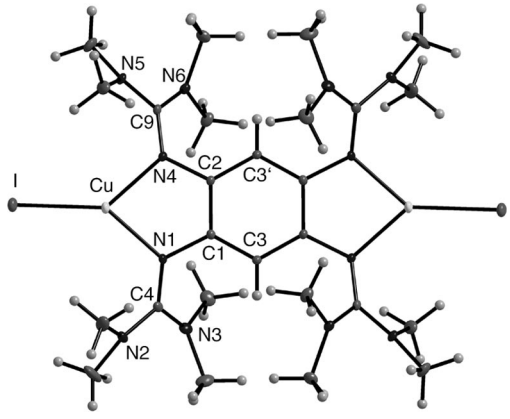

Figure 2. Molecular structure of **3**. Thermal ellipsoids are drawn at the 50% probability level.

in particular showed that a Cu^I coordination polymer is formed. Figure 3 displays a section of the structure of one of the chains containing the oxidized guanidine ligands. The formally dicationic ttmgb ligand units adopt a bisallyl-type structure. Four of the C–C bond lengths are equal and measure 140.7(6) pm. The two allyl parts are connected through two C–C single bonds of 149.2(11) pm. Two adjacent copper atoms within the chains are bound together

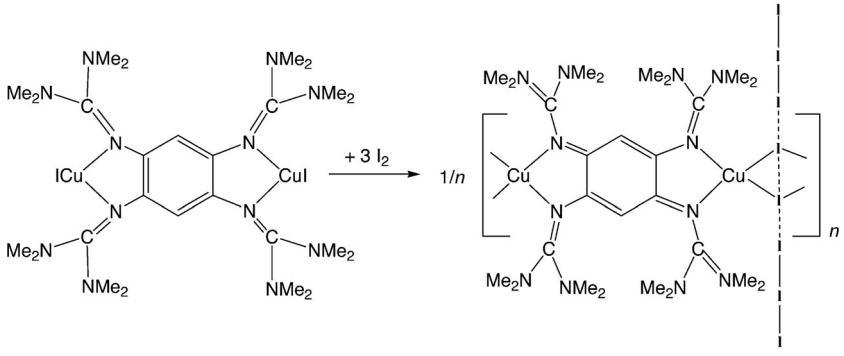

3 **4** (1)

through two bridging iodine atoms, thereby leading to an increase of the coordination number from three in **3** to four in **4**.

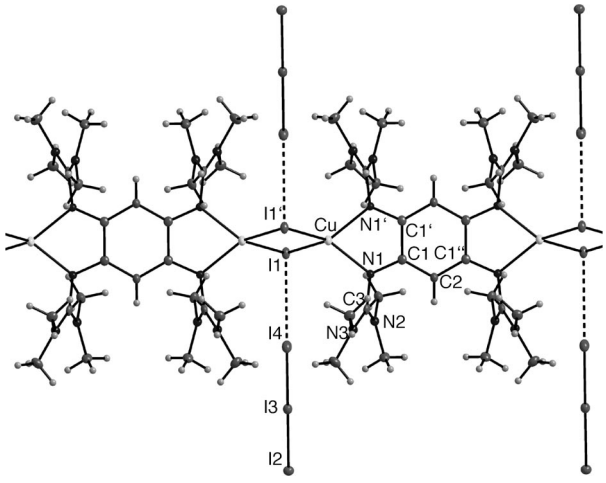

Figure 3. Molecular structure of a fraction of a chain in **4**. Thermal ellipsoids are drawn at the 50% probability level.

This increase can be simply rationalized as follows. The neutral ttmgb ligand is an excellent electron donor and strong base that forms strong coordination bonds with the Cu^{I} ions. Oxidation significantly reduces the basicity and strength of coordination bonds. Consequently, the Cu^{I} ion prefers a higher coordination number. In line with this argument, the Cu–N bond lengths in **4** measure 206.4(4) pm and are thus larger than those in **3** [201.59(18)/201.65(17) pm]. At 79.03(3)°, the Cu–I–Cu bond angles are large, which leads to extremely large Cu···Cu separations of 330.6 pm. For comparison, the Cu–I–Cu angle and Cu···Cu distances in the binuclear complex [{CuI(phen)}$_2$] (phen = phenanthroline) measure 59.96(4)° and 260.9(2) pm, respectively.[17] In [{CuI(hppMe)}$_2$], which features guanidine ligands {hppMe denotes an *N*-methyl-substituted 1,3,4,6,7,8-hexahydro-2*H*-pyrimido[1,2-*a*]pyrimidine (hppH) ligand}, Cu–I–Cu angles of 60.65(8)° are realized.[18] Generally, in the case of polymeric chains with Cu(μ-I)$_2$Cu units, the two Cu ions of each Cu(μ-I)$_2$Cu unit could either belong to a single chain (like in **4**)[19] or to a double chain in which the two chains are connected through the iodide ions.[20] The polymer [(CuI)$_2$(phz)] (phz = phenazine) is an example for the former case.[19a] However, in contrast to the situation in **4**, each Cu is tricoordinated. A more closely related example featuring four-coordinate Cu ions that belong to the same chain (but with sulfur-bonded chelating ligands) is [(CuI)$_2$(tptb)] (tptb = 1,2,4,5-tetra(isopropylthio)benzene, see Scheme 2).[19b] Therein the Cu–I bond lengths and I–Cu–I bond angles were determined to be 261.3(3)/263.8(3) pm and 111.5(1)/112.3(1)°, respectively, which deviates significantly once again from the situation in **4**. What is the reason for this unusual structure of the Cu(μ-I)$_2$Cu units in **4**? Steric repulsion between the guanidino groups of the ttmgb ligands might be one reason. It has been shown that the Cu(μ-I)$_2$Cu units can react flexibly to the steric demands of the ligands. Hence replacement of the phen ligands in [{CuI(phen)}$_2$] by dmphen (dmphen = 2,9-dimethyl-1,10-phenanthroline) leads to binuclear complexes with Cu–I–Cu angles and Cu···Cu separations of 60.38(4)° and 302.4(2) pm, respectively.[17] However, the corresponding parameters for **4** are still larger by far, thereby suggesting the presence of additional effects. One effect that might play a role is the interaction between the two bridging iodine atoms. With 400.8(1) pm, the I···I distance in **4** is significantly shorter than the van der Waals contact distance between two iodine atoms of 420 pm. For comparison, it measures 445.4(2) pm in [{CuI(phen)}$_2$].[17] Interestingly, a bonding interaction is also established between the bridging iodine atoms (I1) and one of the iodine atoms of the I_3^- units. Thus the I1···I4 distance measures only 387.3(2) pm. Consequently, the I_3^- unit is not centrosymmetric. The I3–I4 bond length [287.55(10) pm] is significantly shorter than the I2–I3 bond length [298.99(10) pm]. In an extreme description it could be suggested that I_8^{4-} units are formed, to which the Cu^{I} ions coordinate, so that the compound can be described as $\{[Cu_2(ttmgb)]^{4+}[I_8]^{4-}\}_n$. Figure 4 illustrates the packing of the chains in **4**. The interchain distance is 2.5663 nm. It can be seen that the iodine atoms are also arranged in chains, thereby resulting in a multiladder-type arrangement with a distance of 1.1404 nm between the iodine chains. However, the shortest distance between two I_3^- units (from I2 to the adjacent I_3^-) measures 451.6 pm and is thus already larger than the van der Waals contact distance between two iodine atoms of 420 pm. Another interesting detail is the presence of relatively large empty voids in the crystalline phase. In addition, we studied **4** with X-ray photoelectron spectroscopy (XPS). Figure 5 displays the spectrum in the region of the I 3d, Cu 2p, N 1s and C 1s signals. Two signals at 933.7 and 953.6 eV are visible in the Cu 2p region; these can be assigned to $2p_{3/2}$ and $2p_{1/2}$ of copper in the oxidation state +1.[21] The absence of signals due to Cu^{II}, which should show at around 944 eV for $2p_{3/2}$,[21] clearly confirms that the ttmgb ligand but not the Cu^{I} ions were oxidized by reaction of compound **3** with I_2. Another point worth mentioning is the sharp signals at 620.5 and 632.0 eV due to iodine $3d_{5/2}$ and $3d_{3/2}$. For comparison, the $3d_{5/2}$ signals of the compounds I_2, NaI and CsI_3 were previously reported to appear at 619.9, 618.4 and 618.5/619.7 eV.[22] The energy separation between the two different iodine atoms in I_3^- is too small for detection in our experiment. However, at first glance one would expect the iodine bound to copper to show at different energies. The fact that the energy difference is very small is in line with the idea of an interaction between the iodine atoms and partial delocalization of all four charges over the eight iodine atoms (two I_3^- units and two copper-bound iodides). The N 1s signal can be explained straightforwardly. There are two different sorts of N atoms: the ones from the NMe_2 units and the ones attached to the C_6 ring. They should give rise to two signals with a relative intensity of 2:1. The maximum at 402.2 eV can then be assigned to the NMe_2 groups and the shoulder at 400.5 eV to the N atoms attached to the C_6 ring. The XPS results are thus in full agreement with the results of the single-crystal XRD studies. The

C 1s area is more complicated. According to the molecular structure as derived from the XRD analysis, there should be four different sorts of carbon atoms, which are expected to give rise to four signals with a relative intensity of 8:2:2:1.

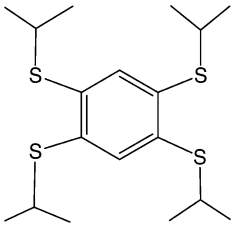

tptb

Scheme 2.

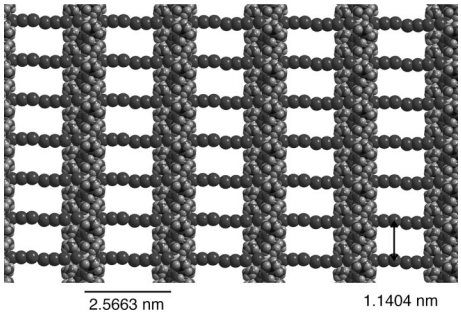

Figure 4. Illustration of the arrangement of the $\{[(CuI)_2(ttmgb)](I_3)_2\}_n$ polymeric chains in the crystal of **4**.

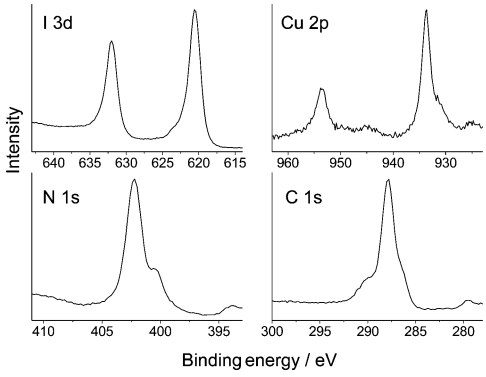

Figure 5. XPS spectra recorded for polymer **4** in the I 3d, Cu 2p, N 1s and C 1s regions.

The Raman spectrum of **4** in the ν(I–I) stretching region of the I_3^- anion (see Figure S1 in the Supporting Information) is dominated by a strong signal at 111 cm^{-1} close to the position expected for the symmetric stretching mode of an I_3^- unit.[23] However, a shoulder appears at 142 cm^{-1}, in proximity to the position measured for the antisymmetric stretching combination of an I_3^- unit. The observation of this signal, which should be Raman silent for a centrosymmetric I_3^- unit, indicates deformation of the I_3^- unit.[24] The other broad signals centred at 221/237 and 340 cm^{-1} are due to overtones of the stretching modes. The IR spectrum of **4** in Nujol shows a strong absorption at 1611 cm^{-1} and a weaker one at 1551 cm^{-1}, which can be assigned to ν(N=C) modes. The Vis/NIR spectrum of **4** is displayed in Figure S2 in the Supporting Information. Groups of absorptions appear at 1934, 2266 (strong), 2294 (strong), 2390, 2453, 2476, 2784 (strong), and 2908 (strong) nm.

The coordination polymer **4** is not soluble without decomposition. Hence it cannot be dissolved in CH_3CN, for example. Interestingly, it can be dissolved in CH_3CN upon addition of 1,10-phenanthroline. If 1,10-phenanthroline dissolved in CH_3CN is added to a suspension of **4** in CH_3CN, the reaction mixture becomes rapidly clear. Orange crystals are formed upon partial solvent removal. A single-crystal XRD analysis showed the crystalline product to be $[Cu(1,10\text{-phenanthroline})_3]^{2+}(I^-)_2$. An illustration of the molecular structure can be found in Figure S3 in the Supporting Information. The structure resembles that previously reported for other salts of this dication {e.g., $[Cu(1,10\text{-phenanthroline})_3]^{2+}(ClO_4^-)_2$}.[25] The oxidation of the copper ions should be accompanied by I_3^- reduction, and reaction should occur according to Equation (2).

The differential scanning calorimetry (DSC) curve of **4** (see Figure S4 in the Supporting Information) shows a sharp irreversible peak at 233 °C. From integration of the peak, the decomposition process can be estimated to be exothermic by around 130 kJ mol^{-1}. Most likely, decomposition is initiated by further oxidation of the copper to the +II oxidation state and iodine reduction. This result confirms that **4** is a metastable intermediate of the redox reaction that leads finally to oxidation of both the ttmgb ligand and copper.

It has been shown in several cases that doping of coordination polymers that consist of electron-donor and -acceptor units with I_2 leads to a remarkable increase in the electrical conductivity of coordination polymers that feature electron-donating ligand units. Hence the one-dimensional coordination polymer $[(CuI)_2(tptb)]_n$ (see Scheme 2 for a visualization of the tptb ligand) is an insulator at room temperature ($\sigma < 10^{-8}$ S m^{-1}) but can be turned into a semiconductor ($\sigma = 5.6 \times 10^{-4}$ S m^{-1}) upon iodide doping.[19b] Unfortunately, like in other cases, the structure of the polymer after iodide doping was not reported. In fact, the copper complexes reported herein represent one of the rare examples for which molecular structures are available both before and after I_2 oxidation of the ligand units. Therefore an analysis of the conductivity of these well-defined compounds is of great interest. Prior to studying the electrical conductivity of **4**, we analyzed salt **1** in which the Cu^I ions are absent. Compound **1** is stable up to temperatures of more than 170 °C according to DSC measurements. As anticipated, the conductivity at room temperature is very low

$$1/n\,\{[(CuI)_2(ttmgb)](I_3)_2\}_n + 6\ phen \xrightarrow{CH_3CN} 2\ [Cu(phen)_3]^{2+} + (ttmgb)^{2+} + 6\ I^- \quad (2)$$

and could not be measured reliably. However, at temperatures above 100 °C the conductivity clearly followed the behaviour of a semiconductor (see Figure 6). The band gap can be estimated with the help of an Arrhenius plot to be 1.8 eV. The absolute conductivity σ is low and amounts to 9×10^{-8} S m^{-1} at 400 K and increases to 5×10^{-7} S m^{-1} at 422 K. The corresponding curve for the coordination polymer **4** is also displayed in Figure 6. Again, semiconductive behaviour was found. The conductivity measurements were repeated several times in both directions with heating and cooling of the samples and proved to be perfectly reproducible. A much lower band gap of 1.05 eV was derived for **4** from the Arrhenius plot. The specific conductivity at 420 K amounts already to around 4.8×10^{-6} S m^{-1}.

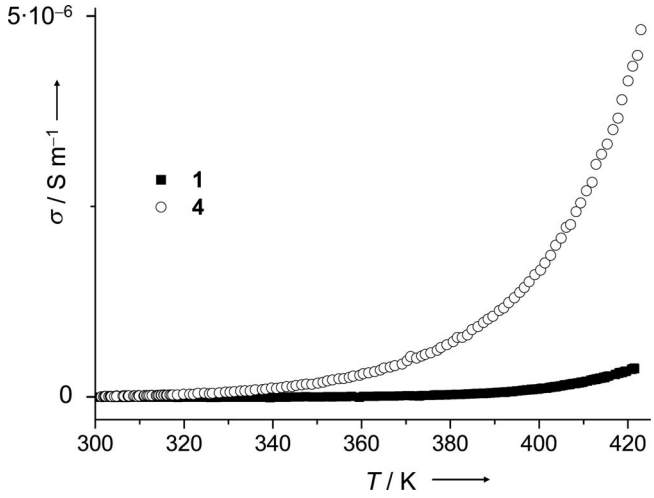

Figure 6. Temperature dependence of the specific conductivity in solid (powder) samples of **1** and **4**.

As already mentioned, polymer **4** can be regarded as a metastable intermediate in the redox reaction that leads finally to oxidation of both the ligand and the copper ions by I_2. This also becomes evident by inspecting the reaction between **2** and the stronger oxidation reagent Br_2. This reaction leads directly to oxidation of both the ligand and the copper ions and formation of the dicationic and binuclear Cu^{II} complex $\mathbf{5}^{2+}$ [see Equation (3)]. Not surprisingly, the C_6 ring gets brominated; similar hydrogen–halide exchange reactions were observed before by us.[8] The dication can be crystallized from the reaction mixture together with $CuBr_4^{2-}$ as counterion. An illustration of the molecular structure is provided in Figure 7. It can be seen that the Cu^{II} ions adopt a coordination that is between tetrahedral and square planar (the dihedral angle between the N–Cu–N and Br–Cu–Br planes being 45.0°).[26] As anticipated, the signals in the NMR spectrum were too broad for detection. We showed for the example complexes $[\{(MeCN)_2Cu\}_2(ttmgb)]$[8] and $[(Cl_2Co)_2(ttmgb)]$[7] that magnetic superexchange in complexes that feature either the dicationic or the neutral ttmgb ligand and square-planar or tetrahedral coordination of electron-rich transition metals is weak (antiferromagnetic coupling). The variations in the C–C bond lengths within the C_6 ring clearly indicate removal of two electrons from the ligand 6π-electron aromatic system. With 149.8(5) pm, the bond lengths C1–C2 and C1′–C2′ qualify as single bonds. Thus the electron acceptor Br_2 pulls out four electrons from complex **2**.

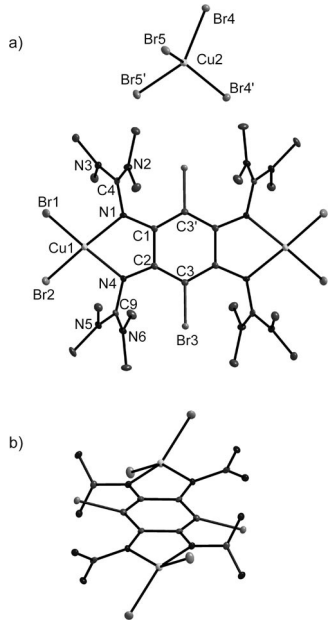

Figure 7. (a) Molecular structure of [**5**]$CuBr_4$. Hydrogen atoms were omitted for the sake of clarity. Thermal ellipsoids are drawn at the 50% probability level. (b) View along the Cu···Cu axis of $\mathbf{5}^{2+}$ highlighting details of the complex geometry. The methyl groups of the ttmgb ligand were omitted for sake of clarity.

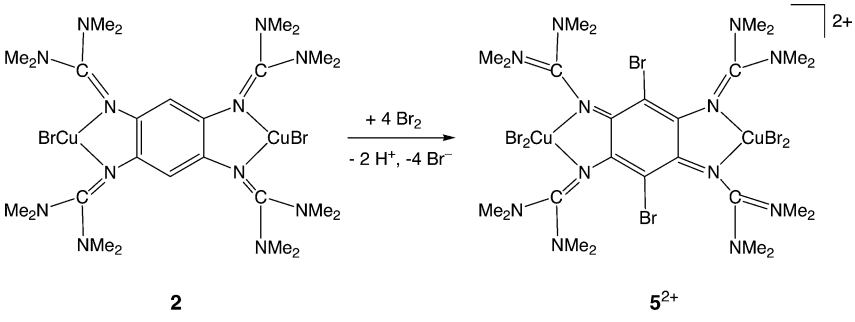

(3)

Conclusion

In this work we reported on the synthesis of the first binuclear Cu^{I} complexes of the guanidine ligand 1,2,4,5-tetrakis(tetramethylguanidino)benzene (ttmgb). These complexes are highly redox-active and amenable to both ligand and Cu^{I} oxidation (representing four-electron donor compounds). The oxidation reactions with Br_2 and I_2 were analyzed and were shown to lead to different products. Hence reaction with Br_2 leads directly to oxidation of both the ligand and the copper ions (four-electron oxidation). A dicationic and binuclear Cu^{II} complex was isolated as the reaction product. On the other hand, reaction with I_2 leads in a first step only to ligand oxidation and formation of the first coordination polymer with incorporated guanidino-functionalized aromatic compounds (GFAs). The black polymer represents an electrical semiconductor with a band gap of around 1 eV and is metastable towards oxidation of copper and reduction of iodine. Its decomposition occurs at around 230 °C. The results reported herein build the basis for future work that concentrates on the analysis of the oxidation reactions of other binuclear Cu^{I} complexes featuring redox-active GFA ligands with the aim of isolating and characterizing redox reaction intermediates (especially products of one-electron ligand oxidations). In the future, research will also be extended to complexes of other metals.

Experimental Section

General: All synthetic work was carried out using standard Schlenk techniques. NMR spectra were measured with a Bruker DPX 200 spectrometer at a temperature of 23 °C and referenced to known standards. IR spectra were recorded with a Bruker Vertex 80v spectrometer. A Perkin–Elmer Lambda 19 spectrometer was used for UV/Vis measurements, and Vis/NIR spectra were obtained with the aid of a Cary 5000 spectrometer. Electrical conductivity measurements were performed on compressed pellets of the respective samples. A standard two-probe setup was used with a constant voltage of 1 V. CuBr and CuI were purchased from Sigma–Aldrich and Strem Chemicals, respectively. The neutral tetraguanidino ligand, ttmgb [tetrakis(tetramethylguanidino)benzene] was synthesized as described earlier.[6]

[(CuBr)$_2$(ttmgb)] (2): The ligand ttmgb (200 mg, 0.377 mmol) was dissolved in CH_3CN. Then CuBr (108 mg, 0.754 mmol) was added. The reaction mixture was heated at reflux for 1 h at 70 °C, and then slowly cooled down to room temp. Complex **2** precipitated upon addition of Et_2O (40 mL). The precipitate was filtered and the product was dried in vacuo, thus leaving product (209 mg) in the form of a pale yellow-green powder (66% yield). $C_{26}H_{50}Br_2Cu_2N_{12}$ (817.66): calcd. C 38.19, H 6.16, N 20.56; found C 37.19, H 6.12, N 20.03. ^{1}H NMR (200.13 MHz, CD_3CN): δ = 2.82 (s, 48 H, CH_3), 5.43 (s, 2 H, Ar-H) ppm. ^{13}C NMR (150.90 MHz, CD_2Cl_2): δ = 160.33 [N*C*(NMe$_2$)$_2$], 134.08 ($C_{arom.}$), 115.32 (CH), 38.02 (CH_3) ppm. IR (CsI): $\tilde{\nu}$ = 3464 (m), 2932 (m), 2881 (m), 2301 (w), 1527 (s), 1474 (s), 1389 (s), 1319 (m), 1273 (m), 1148 (s), 1065 (w), 1024 (s), 955 (w), 892 (m), 864 (w), 798 (m), 575 (w), 471 (m), 416 (m), 375 (m) cm^{-1}. MS (FAB): *m*/*z* (%) = 595 (20) [Cu(ttmgb) + 2H]$^+$, 532 (85) [ttmgb + 2H]$^+$, 531 (63) [ttmgb + H]$^+$, 517 (100) [ttmgb – CH_3 + H]$^+$, 486 (60) [ttmgb – HN(CH_3)$_2$]$^+$. UV/Vis (CH_3CN, $c = 7.78\times10^{-5}$ mol L^{-1}): λ (ε, L mol^{-1} cm^{-1}) = 289 (17735), 327 (14093), 391 (12628) nm. Crystal data for **2**·4CH_3CN: $C_{34}H_{62}Br_2Cu_2N_{16}$, M_r = 981.90, $0.25\times0.15\times0.10$ mm^3, triclinic, space group $P\bar{1}$, lattice constants a = 10.262(2) Å, b = 11.285(2) Å, c = 12.510(3) Å, α = 104.40(3)°, β = 102.89(3)°, γ = 116.88(3)°, V = 1153.3(4) Å^3, Z = 1, $d_{calcd.}$ = 1.414 Mg m^{-3}, θ_{range} = 1.82 to 27.49°. Reflections measured 16580, independent 5237, R_{int} = 0.0551. Final R indices [$I>2\sigma(I)$]: R_1 = 0.0482, wR_2 = 0.1212.

[(CuI)$_2$(ttmgb)] (3): The ligand ttmgb (200 mg, 0.377 mmol) was dissolved in CH_3CN. Then CuI (143 mg, 0.754 mmol) was added. The reaction mixture was heated at reflux for 1 h at 70 °C, and then slowly cooled down to room temp. Complex **2** precipitated upon addition of Et_2O (40 mL). The precipitate was filtered and the product was dried in vacuo, leaving product (260 mg) in the form of a pale-yellow powder (72% yield, without CH_3CN). $C_{26}H_{50}I_2Cu_2N_{12}$ (911.66): calcd. C 34.25, H 5.53, N 18.44. $C_{26}H_{50}Cu_2I_2N_{12}$·$CH_3CN$: calcd. C 35.30, H 5.61, N 19.10; found C 35.74, H 5.64, N 19.42. The experimental data suggest the presence of CH_3CN even after drying in vacuo. ^{1}H NMR (200.13 MHz, CD_3CN): δ = 2.92 (s, 48 H, CH_3), 5.59 (s, 2 H, Ar-H) ppm. ^{13}C NMR (150.90 MHz, CD_2Cl_2): δ = 160.40 [N*C*(NMe$_2$)$_2$], 134.10 ($C_{arom.}$), 114.66 (CH), 37.87 (CH_3) ppm. MS (FAB): *m*/*z* (%) = 975 (4) [Cu_3I_2(ttmgb) + 2H]$^+$, 912 (7) [(CuI)$_2$(ttmgb) + 2H]$^+$, 785 (16) [Cu_2I(ttmgb) + 2H]$^+$, 721 (16) [(CuI)(ttmgb) + H]$^+$, 593 (35) [Cu(ttmgb)]$^+$, 595 (16) [Cu(ttmgb) + 2H]$^+$, 531 (68) [ttmgb + H]$^+$, 530 (92) [ttmgb], 486 (94) [ttmgb – HN(CH_3)$_2$], 432 (26) [ttmgb – H_2C{N(CH_3)$_2$}$_2$], 417 (100) [ttmgb-C(NH)(NMe$_2$)$_2$]$^+$. UV/Vis (CH_3CN, $c = 22.25\times10^{-5}$ mol L^{-1}): λ (ε, dm^3 mol^{-1} cm^{-1}): 242 (32483), 288 (14654), 327 (11120), 391 (10033) nm. IR (CsI): $\tilde{\nu}$ = 3465 (m), 2930 (m), 2880 (m), 2359 (w), 1533 (s), 1475 (s), 1403 (s), 1319 (m), 1156 (s), 1026 (s), 881 (m), 715 (m), 568 (m), 414 (m), 371 (m) cm^{-1}. Crystal data for **3**·4CH_3CN: $C_{34}H_{62}Cu_2I_2N_{16}$, M_r = 1075.88, $0.40\times0.30\times0.30$ mm^3, triclinic, space group $P\bar{1}$, lattice constants a = 10.532(2) Å, b = 11.271(2) Å, c = 12.285(3) Å, α = 105.00(3)°, β = 104.02(3)°, γ = 113.41(3)°, V = 1190.7(4) Å^3, Z = 1, $d_{calcd.}$ = 1.500 Mg m^{-3}, θ_{range} = 1.86 to 33.00°. Reflections measured 35811, independent 8970, R_{int} = 0.0421. Final R indices [$I>2\sigma(I)$]: R_1 = 0.0323, wR_2 = 0.0856.

[(CuI)$_2$(ttmgb)](I$_3$)$_2$ (4): An excess amount of I_2 (50 mg, 0.198 mmol) was added to a solution of **3** (90 mg, 0.099 mmol) in CH_3CN (10 mL). The reaction mixture was stirred for a period of 1 h at room temp. Partial removal of the solvent led to formation of a precipitate, which was filtered and dried in vacuo. The product was obtained in the form of a black solid (66 mg, 40% yield). $C_{26}H_{50}Cu_2I_8N_{12}$ (1673.08): calcd. C 19.20, H 3.22, N 9.95; found C 19.51, H 3.16, N 10.41. IR (CsI): $\tilde{\nu}$ = 3487 (m), 2931 (w), 2374 (w), 1608 (m), 1479 (m), 1477 (m), 1393 (s), 1308 (s), 1169 (w), 1067 (w), 788 (m), 408 (s), 356 (m) cm^{-1}. MS (FAB): *m*/*z* (%): 1224 (17) [(CuI)$_2$(ttmgb) + H – 2C{N(CH_3)$_2$}$_2$]$^+$, 1037 (21) [Cu_2I_3-(ttmgb)]$^+$, 911 (19) [(CuI)$_2$(ttmgb) + H]$^+$, 849 (21) [(ttmgb) + 2H]$^+$, 750 (19) [(CuI$_2$)(ttmgb) + 3H – C{N(CH_3)$_2$}$_2$]$^+$, 659 (38) [ttmgb + I + 2H]$^+$, 531 (100) [ttmgb + H]$^+$, 486 (60) [ttmgb – HN(CH_3)$_2$]$^+$. Crystal data for **4**: $C_{13}H_{25}CuI_4N_6$, M_r = 836.54, $0.18\times0.10\times0.10$ mm^3, monoclinic, space group *C*2/*m*, lattice constants a = 16.001(3) Å, b = 11.404(2) Å, c = 14.383(3) Å, β = 115.16(3)°, V = 2375.5(10) Å^3, Z = 4, $d_{calcd.}$ = 2.339 Mg m^{-3}, θ_{range} = 1.56 to 27.59°. Reflections measured 22290, independent 2878, R_{int} = 0.0726. Final R indices [$I>2\sigma(I)$]: R_1 = 0.0393, wR_2 = 0.0892.

5[CuBr$_4$]: A solution of Br_2 (25 mg, 159 μmol) in CH_3CN (1 mL) was added dropwise to a solution of [(CuBr)$_2$(ttmgb)] (65 mg, 79.5 μmol) in CH_3CN (10 mL). The reaction mixture was stirred for a

period of 3 h at room temp. Subsequently the solvent was removed, so that only around 5 mL remained. Complex **5**[$CuBr_4$] was precipitated by addition of Et_2O (40 mL), then filtered and dried in vacuo. A yield of 44 mg (29.2 μmol, 36.7%) was obtained. Crystals suitable for an XRD analysis can be grown from concentrated CH_3CN solutions. Elemental analysis of the dried powder: $C_{26}H_{48}Br_{10}Cu_3N_{12}$ (1518.42): calcd. C 20.57, H 3.19, N 11.07; found C 20.77, H 3.40, N 11.00. Elemental analysis of the crystals **5**[$CuBr_4$]·2CH_3CN: $C_{30}H_{54}Br_{10}Cu_3N_{14}$ (1600.53): calcd. C 22.51, H 3.40, N 12.25; found C 22.51, H 3.45, N 12.20. IR (CsI): $\tilde{\nu}$ = 3025 (w), 2976 (m), 2939 (m), 2798 (w), 1640 (vs), 1507 (s), 1447 (m), 1388 (s), 1362 (s), 1279 (s), 1173 (vs), 1058 (s), 1010 (m), 895 (m), 843 (m), 794 (m), 720 (m), 676 (w), 646 (w), 590 (m) cm^{-1}. MS-FAB: *m*/*z* (%) = 644.0 (100) $[C_6Br_2\{NC(NMe_2)_2\}_4 - C_2H_4N]^+$, 688.0 (78) $[C_6Br_2\{NC(NMe_2)_2\}_4 + 2H]^+$, 751.2 (6) [Cu + C_6Br_2-$\{NC(NMe_2)_2\}_4$ + 2H]$^+$, 830.9 (28) [CuBr + $C_6Br_2\{NC(NMe_2)_2\}_4$ + 2H]$^+$, 831.8 (42) [CuBr + $C_6Br_2\{NC(NMe_2)_2\}_4$ + 3H]$^+$. UV/Vis (CH_3CN, $c = 9.4 \times 10^{-5}$ mol L^{-1}): λ (ε, L mol^{-1} cm^{-1}) = 270 (37840), 424 (26566), 636 (2614), 320 (20213) nm. Crystal data for **5**[$CuBr_4$]·2CH_3CN: $C_{30}H_{54}Br_{10}Cu_3N_{14}$, M_r = 1600.52, $0.30 \times 0.25 \times 0.15$ mm^3, monoclinic, space group *C*2/*c*, lattice constants *a* = 29.067(6) Å, *b* = 12.944(3) Å, *c* = 14.165(3) Å, β = 107.58(3)°, *V* = 5081(2) $Å^3$, *Z* = 4, $d_{calcd.}$ = 2.093 Mg m^{-3}, θ_{range} = 1.47 to 27.55°. Reflections measured 46670, independent 5863, R_{int} = 0.0968. Final *R* indices [$I > 2\sigma(I)$]: R_1 = 0.0363, wR_2 = 0.0893.

X-ray Crystallographic Study: Suitable crystals were taken directly out of the mother liquor, immersed in perfluorinated polyether oil and fixed on top of a glass capillary. Measurements were made on a Nonius–Kappa CCD diffractometer with a low-temperature unit using graphite-monochromated Mo-K_α radiation. The temperature was set to 100 K. The data collected were processed using the standard Nonius software.[27] All calculations were performed using the SHELXT-PLUS software package. Structures were solved by direct methods with the SHELXS-97 program and refined with the SHELXL-97 program.[28,29] Graphical handling of the structural data during solution and refinement was performed with XPMA.[30] Atomic coordinates and anisotropic thermal parameters of non-hydrogen atoms were refined by full-matrix least-squares calculations.

CCDC-749677 (for **2**), -749676 (for **3**), -749678 (for **4**), -754895 {for [Cu(1,10-phenanthroline)$_3$]$^{2+}$(I^-)$_2$} and -759376 (for **5**[$CuBr_4$]) contain the supplementary crystallographic data for this paper. These data can be obtained free of charge from The Cambridge Crystallographic Data Centre via www.ccdc.cam.ac.uk/data_request/cif.

Supporting Information (see also the footnote on the first page of this article): It includes tables with selected structural parameters from single-crystal XRD studies; Raman und UV/Vis spectra as well as the DSC curve measured for coordination polymer **4**; illustration of the structure of [Cu(phen)$_3$]I_2 from an XRD analysis. UV/Vis and IR spectra of [**5**]$CuBr_4$.

Acknowledgments

The authors gratefully acknowledge continuous financial support by the Deutsche Forschungsgemeinschaft (DFG). N. W. and J. B. especially thank the DFG for support through SFB 813 at the University of Bonn. We thank Prof. Dr. Zharnikov for the XPS measurements.

[1] a) P. Nguyen, P. Gmez-Elipe, I. Manners, *Chem. Rev.* **1999**, *99*, 1515–1548; b) G. R. Whittell, I. Manners, *Adv. Mater.* **2007**, *19*, 3439–3468.
[2] C. Janiak, *Dalton Trans.* **2003**, 2781–2804.
[3] B. Moulton, M. J. Zaworotko, *Chem. Rev.* **2001**, *101*, 1629–1658.
[4] a) Special Issue on Molecular Conductors, in: *Chem. Rev.* (Guest Ed.: P. Batail), **2004**, vol. 104, pp. 4887–5782; b) Special Issue on Organic Frameworks, in: *Chem. Soc. Rev.* (Guest Eds.: J. Long, O. Yaghi), **2009**, vol. 38, pp. 1201–1508.
[5] See, for example: a) M. Munakata, T. Kuroda-Sowa, M. Maekawa, A. Honda, *J. Chem. Soc., Dalton Trans.* **1994**, 2771–2775; b) K. Biradha, M. Aoyagi, M. Fujita, *J. Am. Chem. Soc.* **2000**, *122*, 2397–2398; c) A. J. Blake, N. R. Brooks, N. R. Champness, M. Crew, A. Deveson, D. Fenske, D. H. Gregory, L. R. Hanton, P. Hubberstey, M. Schröder, *Chem. Commun.* **2001**, 1432–1433; d) Y. Chen, H.-X. Li, D. Liu, L.-L. Liu, N.-Y. Li, H.-Y. Ye, Y. Zhang, J.-P. Lang, *Cryst. Growth Des.* **2008**, *8*, 3810–3816.
[6] A. Peters, E. Kaifer, H.-J. Himmel, *Eur. J. Org. Chem.* **2008**, 5907–5914.
[7] V. Vitske, C. König, O. Hübner, E. Kaifer, H.-J. Himmel, *Eur. J. Inorg. Chem.* **2010**, 115–126.
[8] A. Peters, C. Trumm, M. Reinmuth, D. Emeljanenko, E. Kaifer, H.-J. Himmel, *Eur. J. Inorg. Chem.* **2009**, 3791–3800.
[9] F. T. Edelmann, *Adv. Organomet. Chem.* **2008**, *57*, 183–352.
[10] S. Herres-Pawlis, *Nachr. Chem.* **2009**, *57*, 20–23.
[11] S. Pohl, M. Harmjanz, J. Schneider, W. Saak, G. Henkel, *J. Chem. Soc., Dalton Trans.* **2000**, 3473–3479.
[12] D. Petrovic, L. M. R. Hill, P. G. Jones, W. B. Tolman, M. Tamm, *Dalton Trans.* **2008**, 887–894.
[13] C. Würtele, E. Gaoutchenova, K. Harms, M. C. Holthausen, J. Sundermeyer, S. Schindler, *Angew. Chem.* **2006**, *118*, 3951–3954; *Angew. Chem. Int. Ed.* **2006**, *45*, 3867–3869.
[14] a) D. Maiti, D.-H. Lee, K. Gaoutchenova, C. Würtele, M. C. Holthausen, A. A. N. Sarjeant, J. Sundermeyer, S. Schindler, K. D. Karlin, *Angew. Chem.* **2008**, *120*, 88–91; *Angew. Chem. Int. Ed.* **2008**, *47*, 82–85; b) M. P. Lanci, V. V. Smirnov, C. J. Cramer, E. V. Gauchenova, J. Sundermeyer, J. P. Roth, *J. Am. Chem. Soc.* **2007**, *129*, 14697–14709.
[15] A. Neuba, R. Haase, M. Bernard, U. Flörke, S. Herres-Pawlis, *Z. Anorg. Allg. Chem.* **2008**, *634*, 2511–2517.
[16] For a detailed analysis of the dynamical behaviour of some bisguanidine metal complexes, see: M. Reinmuth, U. Wild, D. Rudolf, E. Kaifer, M. Enders, H. Wadepohl, H.-J. Himmel, *Eur. J. Inorg. Chem.* **2009**, 4795–4808.
[17] P. C. Healy, C. Pakawatchai, A. H. White, *J. Chem. Soc., Dalton Trans.* **1985**, 2531–2539.
[18] S. H. Oakley, M. P. Coles, P. B. Hitchcock, *Inorg. Chem.* **2004**, *43*, 5168–5172.
[19] See, for example: a) M. Munakata, T. Kuroda-Sowa, M. Maekawa, A. Honda, *J. Chem. Soc., Dalton Trans.* **1994**, 2771–2775; b) T. Okubo, T. Ohrui, M. Kondo, S. Kitagawa, H. Matsuzaka, *Synth. Met.* **1999**, *102*, 1464–1465.
[20] For the second possibility, see for example: a) Y. Chen, H.-X. Li, D. Liu, L.-L. Liu, N.-Y. Li, H.-Y. Ye, Y. Zhang, J.-P. Lang, *Cryst. Growth Des.* **2008**, *8*, 3810–3816; b) H. J. Kim, M. R. Song, S. Y. Lee, J. Y. Lee, S. S. Lee, *Eur. J. Inorg. Chem.* **2008**, 3532–3539.
[21] See, for example: a) H. Yang, J. Lin, J. Chen, X. Zhu, S. Gao, R. Cao, *Cryst. Growth Des.* **2008**, *8*, 2623–2625; b) Y.-H. Wen, J.-K. Cheng, J. Zhang, Z.-J. Li, Y. Kang, Y.-G. Yao, *Inorg. Chem. Commun.* **2004**, *7*, 1120–1123; c) Y. Feng, Z. Han, J. Peng, X. Hao, *J. Mol. Struct.* **2005**, *734*, 171–176; d) Y.-H. Sun, J.-H. Yu, X.-J. Jin, J.-F. Song, J.-Q. Xu, L. Ye, *Inorg. Chem. Commun.* **2006**, *9*, 1087–1090.
[22] P. M. A. Sherwood, *J. Chem. Soc. Faraday Trans. 2* **1976**, *72*, 1805–1820.

[23] a) W. Kiefer, H. J. Bernstein, *Chem. Phys. Lett.* **1972**, *16*, 5–9; b) K. Kaya, N. Mikami, Y. Udagawa, M. Ito, *Chem. Phys. Lett.* **1972**, *16*, 151–153.
[24] T. Kawamoto, M. Ashizawa, M. Aragaki, T. Mori, T. Yamamoto, H. Tajima, H. Kitagawa, T. Mitani, Y. Misaki, K. Tanaka, *Phys. Rev. B* **1999**, *60*, 4635–4645.
[25] O. P. Anderson, *J. Chem. Soc., Dalton Trans.* **1973**, 1237–1241.
[26] Similar geometries were observed in salts containing the $CuBr_4^{2-}$ ion and were explained by ligand–ligand repulsion. See, for example: H. Place, R. D. Willett, *Acta Crystallogr., Sect. C* **1988**, *44*, 34–38.
[27] DENZO-SMN, Data processing software, Nonius **1998**; ttp://www.nonius.com.
[28] a) G. M. Sheldrick, *SHELXS-97*, *Program for Crystal Structure Solution*, University of Göttingen, **1997**; http://shelx.uni–ac.gwdg.de/SHELX/index.html; b) G. M. Sheldrick, *SHELXL-97*, *Program for Crystal Structure Refinement*, University of Göttingen, **1997**; http://shelx.uni-ac.gwdg.de/SHELX/index.html.
[29] *International Tables for X-ray Crystallography*, vol. 4, Kynoch Press, Birmingham, UK, **1974**.
[30] L. Zsolnai, G. Huttner, *XPMA*, University of Heidelberg, **1994**; http://www.uni-heidelberg.de/institute/fak12/AC/huttner/software/software.html.

Received: January 4, 2010
Published Online: March 19, 2010

